Crystallography of Directionally Solidified Magnesium Alloy AZ91

KETIL PETTERSEN and NILS RYUM

The crystallographic direction of growth in directionally solidified magnesium alloy AZ91 has been studied by TEM and EBSP techniques in SEM. The main direction of growth is found to be $\langle 11\bar{2}0\rangle$. The dendrites have sixfold symmetry around the main direction, with secondary arms lying along the traces of the (0001), $(1\bar{1}01)$, and $(\bar{1}101)$-planes, respectively. The secondary arms lying in the basal plane are crystallographically of the same type as the main direction: $\langle\bar{1}2\bar{1}0\rangle$ and $\langle 2\bar{1}\bar{1}0\rangle$.

I. INTRODUCTION

THE crystallographic directions of dendritic solidification have been studied and reported for a number of metals. Extensive information is given in References 1 through 5. It is generally believed that the preferred direction of growth is the same for metals of the same lattice system. For fcc metals, these are the $\langle 100\rangle$-directions.[4] For hcp-metals, it is always stated that $\langle 10\bar{1}0\rangle$ are the directions of dendrite growth,[1–4] even though this has been established firmly only for high purity Zn.[6] For nonmetallic materials with hcp-symmetry, Kurz and Fisher[5] reported a $\langle 10\bar{1}0\rangle$-direction for H_2O and $\langle 0001\rangle$-direction for $Co_{17}Sm_2$. This shows that the preferred directions of growth are not the same for different hcp-materials. The general principle for all kinds of materials is that the direction of dendritic growth is the axis of a pyramid whose sides are the closest packed planes with which a pyramid can be formed.[1,4] This is based on the fact that the direction perpendicular to the closest packed planes is the slowest growing direction (Bravai's rule). However, the most closely packed planes in hcp-materials depend on the c/a ratio, and, because the c/a ratio may differ to a great extent among the hcp-materials, the dendritic direction also may differ among the hcp-materials.

In the present investigation, the crystallography of dendritic solidification of the magnesium alloy AZ91 has been examined. This is done by directional solidification of the alloy and by subsequent study of the resulting microstructure.

II. EXPERIMENTAL PROCEDURE

A. *Alloy*

In the present study, an industrial magnesium alloy was examined. The composition of the alloy was 9.1 wt pct Al, 0.81 wt pct Zn, 0.27 wt pct Mn, 0.01 wt pct Si, other impurities <0.01 wt pct, and balance Mg. By thermal analyses, the liquidus temperature was found to be 599 °C and the eutectic temperature 428 °C. Thus, the solidification range was 171 K.

KETIL PETTERSEN, Research Scientist, is with the Division of Metallurgy, SINTEF, N-7034 Trondheim, Norway. NILS RYUM, Professor, is at the Institute of Metallurgy, The Norwegian Institute of Technology, N-7034 Trondheim, Norway.

Manuscript submitted March 4, 1988.

B. *Solidification*

The solidification was performed in a 110 × 110 × 200 mm^3 mold with insulated sides and top and a removable steel bottom plate. The principles of this method are described in Reference 5. The liquid metal was held in a crucible at 700 °C, and poured manually into the mold under the protection of SF_6. After pouring, the insulating top plate was put on, and the protection with SF_6 continued through a tube in the top plate. The steel bottom plate was cooled by direct water spraying, but, after about 30 seconds, the bottom plate was withdrawn and direct water cooling of the casting occurred. Thermocouples were positioned at 29, 55, 70, and 97 mm above the bottom to record the temperature during the solidification process. The temperatures were recorded at a rate of 3 s^{-1} by means of a computer. Temperature-time graphs from the investigated casting are shown in Figure 1.

From the exact thermocouple positions and the information from Figure 1, the thermal conditions of the casting were found. The macroscopic temperature gradient, $G = \Delta T/\Delta X$, was found as the difference between the thermocouple readings at a specified point of time. For the investigated casting, G varied from 3 to 1.5 K/mm at the liquidus temperature, the gradient was steepest at the bottom of the casting, and decreased upward. The rate of solidification is related to the velocities of the liquidus and solidus isotherms. The liquidus isotherm propagated at a velocity of 0.7 to 0.4 mm/second, fastest at the bottom of the casting. The eutectic isotherm velocity was quite constant in the measured zone at about 0.16 mm/second. The local solidification time was calculated for each thermocouple position. Results from several other similar castings with somewhat different thermocouple positions also are included in this calculation. Here, Δt is the time between the liquidus and eutectic temperatures. A linear relationship between Δt and the position in the casting (X) was found:

$$\Delta t = (3.93X - 82)\text{sec}, \qquad X \text{ in mm}$$

The specimens for the metallographic investigations were taken from a position about 90 mm from the bottom chill face and had a local solidification time of about 270 seconds (4.5 minutes).

This casting technique resulted in a columnar zone of about 120 mm from the bottom and upward. The top

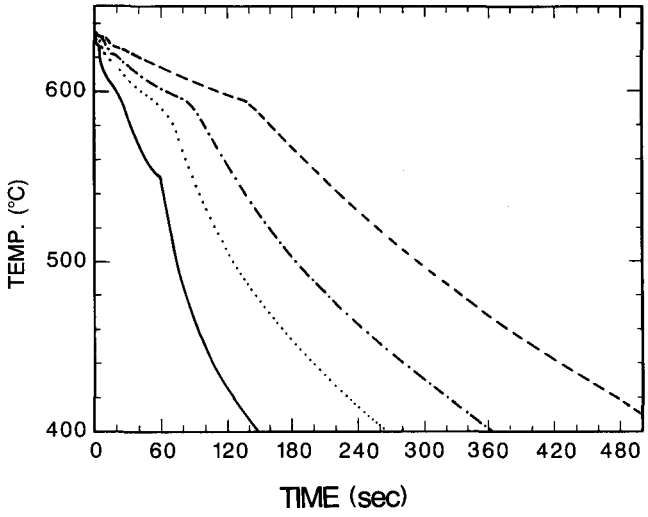

Fig. 1—Temperature-time recordings for the investigated casting. Thermocouple positions are, from left to right, 29 mm, 55 mm, 70 mm, and 97 mm above the bottom of the casting.

region of the casting had a coarse-grained equiaxed structure.

C. *Metallography*

The material for the metallographic investigation was taken from the upper part of the columnar zone. The specimens were wet ground and mechanically polished, and finally etched in a solution of 1 ml HNO_3, 20 ml acetic acid, 60 ml ethylenglycol, and 20 ml H_2O for 20 seconds. The microstructure was studied in the light microscope and in SEM. Some of the pictures from this investigation are shown in Figure 2.

D. *TEM Investigation*

To investigate the crystallographic direction of solidification, a first attempt was made by standard thin foil technique in TEM. Foils were prepared normal to the growth direction. Because of the coarse secondary particles, it was difficult to prepare thin foils in the as-cast condition. This problem was overcome by a homogenization heat treatment at 410 °C for 48 hours. Light microscopy inspection revealed that most of the particles (all of the coarse particles) were dissolved, while no changes had occurred to the columnar structure. Thin foils now could be produced without problems by the standard double jet technique in a solution of 5 pct HNO_3, in ethanol at 0 °C and 5 V. Great care was taken during the cutting of the foils to keep the foils in the plane normal to the growth direction of solidification. This technique gives information about the main direction of dendritic growth, but it was not possible to find the directions of the dendrite arms. An indexed TEM diffraction pattern is shown in Figure 3.

E. *EBSP Investigation (Electron Back Scattered Patterns)*

The EBSP technique is described thoroughly by Dingley.[7] With this technique one obtains, in SEM, a diffraction pattern from a small volume of material ($<1\ \mu m^3$). Thus, particles do not present a problem when recording the diffraction patterns. In practice, one first photographs the specimen in the SEI-mode when mounted horizontally in SEM. One then has to tilt the specimen 75 deg to obtain the EBSP pattern. If one keeps track of the position during tilting, it is possible to index the crystallographic directions of the solidification structure in the specimen. To obtain good results, the specimens cannot be mechanically deformed. Thus, the mechanically polished specimens have to be etched rather heavily. A solution of 10 ml HNO_3, 30 ml acetic acid, 40 ml H_2O, and 120 ml ethanol was used, and the etching time was 45 seconds.

III. RESULTS AND DISCUSSION

Figure 2 shows some light microscope and SEM micrographs from the typical directionally solidified structure. Figure 2(a) is taken parallel to the solidification direction and shows a longitudinal section through the columnar dendrites. Figures 2(b) and (c) are from the transverse section and show the shape of the dendrites in a direction normal to their growth direction. The characteristic features of this structure are small dendrite trunks with sixfold symmetry and a long-range arrangement of the trunks along one of these sixfold directions. By successively grinding and polishing, while keeping track of the positions, it was revealed that the shape was the same downward through the casting, parallel to the growth direction. The width and length of the arms varied to some extent, but the shape of the dendrites is invariant along the growth direction. On the basis of these observations, it has not been possible to find the exact direction of the individual secondary dendrite arms. This will be studied in a further investigation, but here the effort is concentrated on studying the primary direction.

The TEM-diffraction pattern in Figure 3 was obtained with the electron beam parallel to the growth direction. As can be seen, the foil normal is close to the $\langle 11\bar{2}0\rangle$-direction. Several foils were examined with the same result. The columnar dendrites in the investigated specimens were clearly visible from macroetching. This made it relatively simple to control the direction when the specimens were prepared further, and no great deviation from the correct angle could result from the preparation. The total uncertainty in orientation of the foil, from preparation and mounting the foils into the TEM, is about 5 deg. The foils were mounted in a double-tilt stage. The tilt-angle from direct mounting of the foil to the nearest $\langle 11\bar{2}0\rangle$-zone always was less than 5 deg. This demonstrates quite clearly that $\langle 11\bar{2}0\rangle$ is the dendrite stem direction in this alloy. This is different from previous results on high purity zinc.[6] The difference in direction between what is found in this work, compared to the work of Weinberg and Chalmers on zinc, is an angle of 30 deg, which is far beyond experimental errors.

In an attempt to determine the directions of the dendrite arms, specimens were investigated by the EBSP technique. Figure 4 shows some results from this work. These pictures show that the dendrite trunks are lying on line along the basal plane, with arms in the same plane. The other dendrite arms lie in the $(10\bar{1}1)$-planes. The

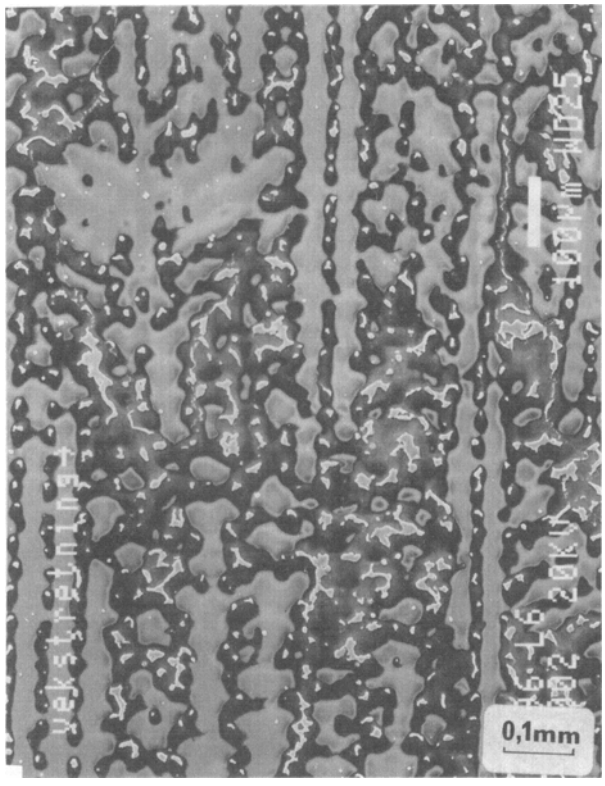

(*a*)

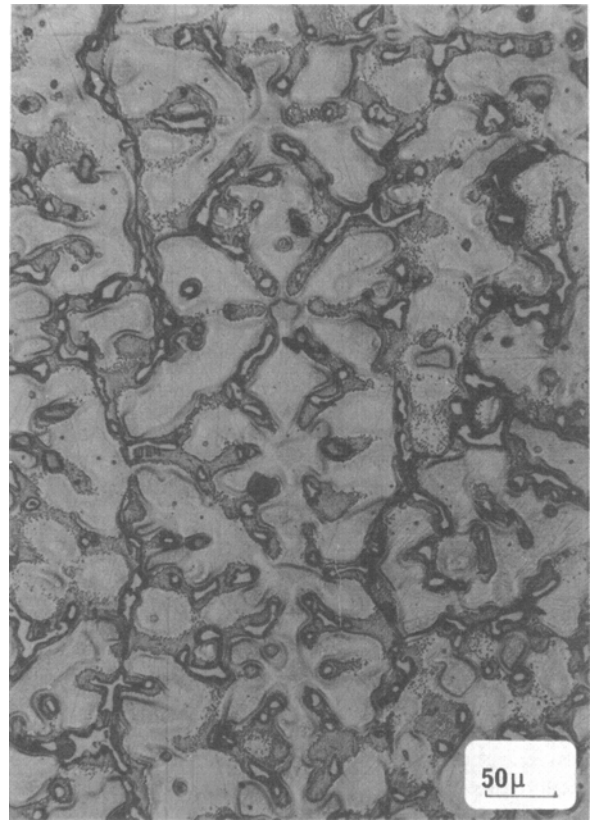

(*c*)

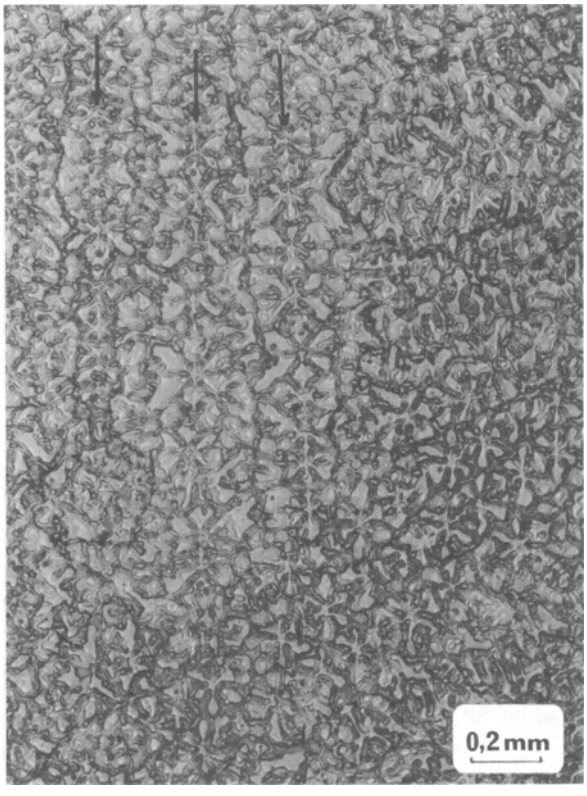

(*b*)

Fig. 2—(*a*) SEM micrograph of a longitudinal section through the casting. The columnar dendrites are lying in the plane of the section, and the individual secondary dendrite arms have grown together to form continuous bands; (*b*) and (*c*) are light microscope micrographs from a transverse section. Notice the long-range arrangement along one of the arm directions. This is clearly seen in (b), where some of these alignments are pointed out.

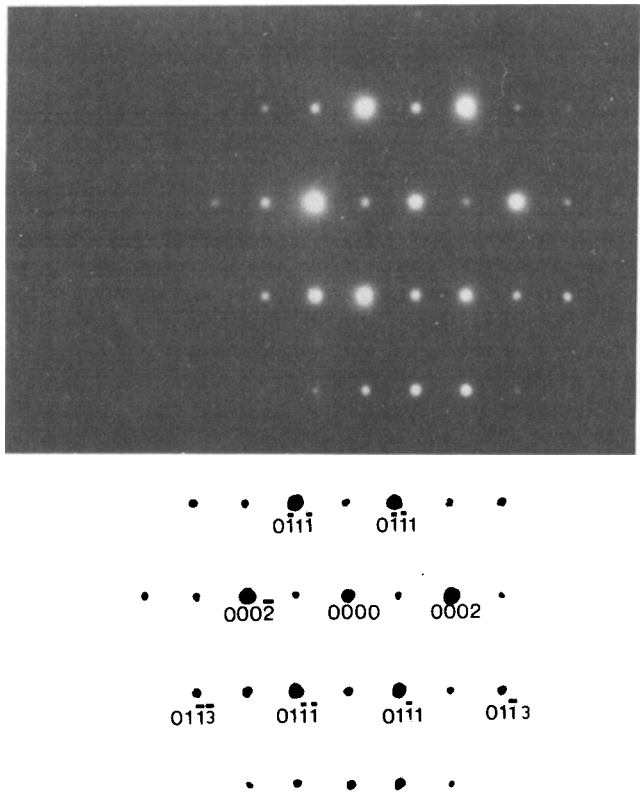

Fig. 3 — TEM-diffraction pattern from a foil taken from the transverse section, with the electron beam along the growth direction. The indexing of the pattern shows a $\langle 11\bar{2}0\rangle$-zone.

direction of the trunk of the dendrites, *i.e.*, the direction of the dendritic growth, is verified to be the $\langle 11\bar{2}0\rangle$-direction.

In the SEM, it was possible to tilt the specimens so that the dendrites could be observed also on the side of the specimen which was parallel to the solidification direction. It was always found that the longitudinal direction of the dendrites was parallel to the solidification direction. This clearly shows that the investigated alloy AZ91 solidifies in the $\langle 11\bar{2}0\rangle$-direction.

The $\langle 11\bar{2}0\rangle$-directions are lying in the basal plane, and the angle between the equivalent directions is 60 deg. Since two of the secondary dendrite arms are lying along the trace of the basal plane, it is reasonable to assume that these secondary arm directions also are $\langle 11\bar{2}0\rangle$-directions.

This also gives an explanation of how the dendrites come to grow on one line along the trace of the basal plane. Dendrites of the $\langle 11\bar{2}0\rangle$-orientation will grow faster than dendrites of other orientations; secondary dendrite arms will grow and also develop tertiary arms. These tertiary arms have the same direction as the original primary dendrite and will continue to grow into a new primary dendrite stalk, aligned with the original stalk in

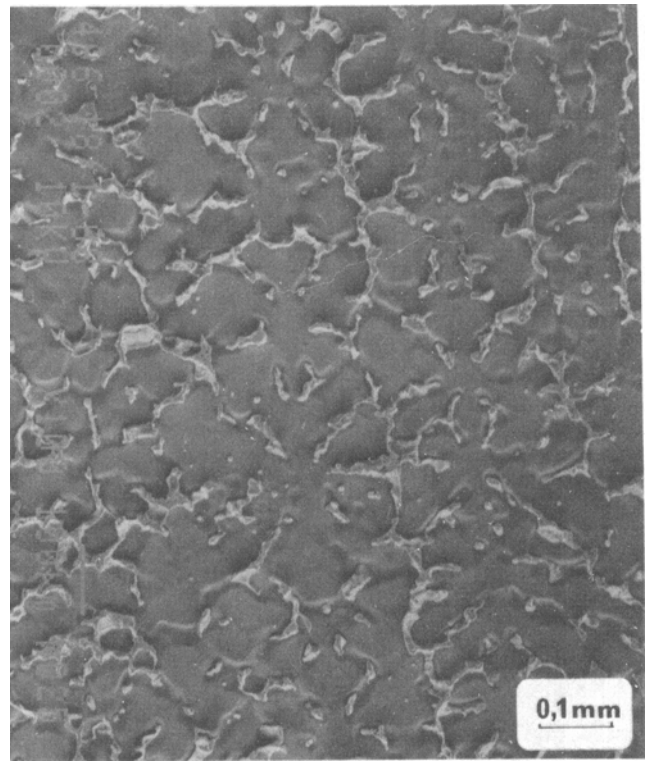

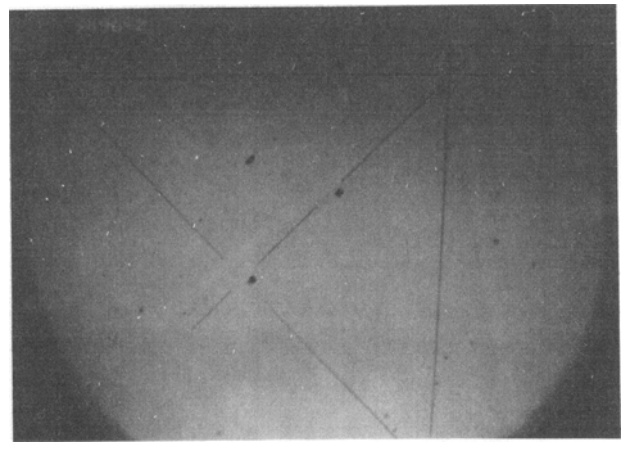

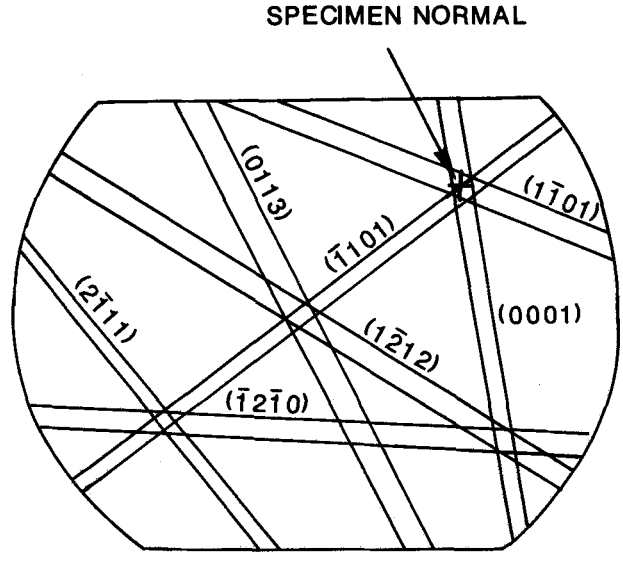

Fig. 4 — SEM micrograph from a transverse section, with an indexed EBSP below. The plane normal is $\langle 11\bar{2}0\rangle$, and the arm directions are lying along the traces of the (0001) and (10$\bar{1}$1)-planes, respectively. The long-range arrangement of the structure is seen to lie along the basal plane.

the basal plane. By continuing this process, a structure like the one shown in Figures 2(b) and (c) will be the result. Similar effects also have been observed in other metal alloys.[8,9] As pointed out by Bower, Brody, and Flemings,[9] there is only one primary dendrite stalk in each grain, and the observed structure is a result of higher order arms branching from one primary stalk. When this branching preferably goes in one direction, the observed dendrite stalks will be lined up along this direction. Figure 5 illustrates this for the arm directions lying in the basal plane.

This process of branching with a resulting alignment of the dendrites is possible also in the directions along the $(10\bar{1}1)$-planes. However, this is not observed in this investigation, where all the long-range alignment is lying in the basal plane. The conclusion to be drawn from this is that the directions in the basal plane are more preferable growth directions than the directions in the $(10\bar{1}1)$-plane.

However, this will not influence the structure of the individual dendrites in a dramatic way. There, one finds a primary stalk and secondary arms. These secondary arms seem to grow together to form planes in the structure. This is illustrated in Figure 6, where the planes of the dendrite arms are drawn, and the directions of the individual secondary arms in the basal plane are indicated. These secondary arm directions are not observed for the arms in the $(1\bar{1}01)$-type planes.

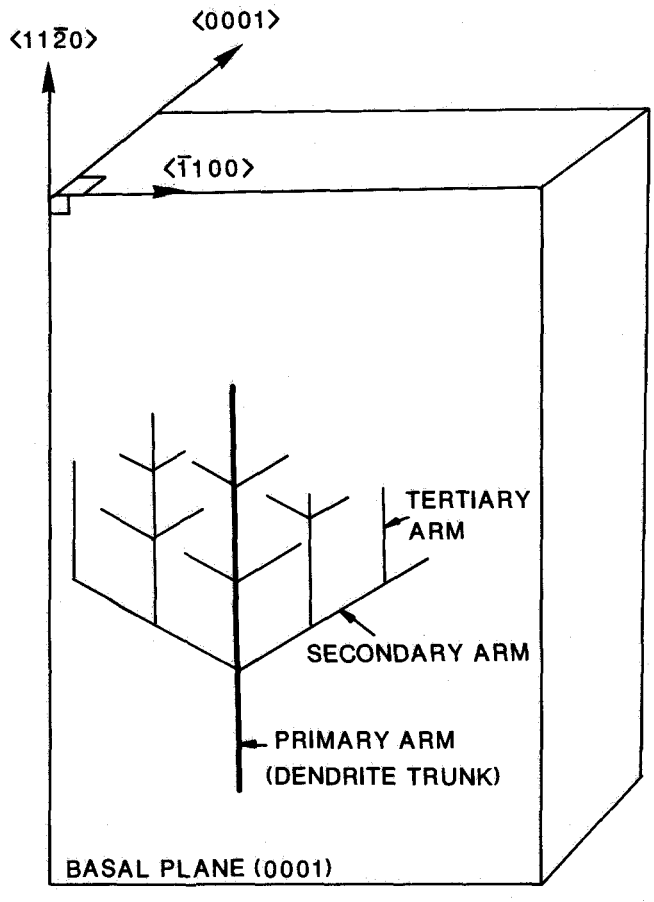

Fig. 5—The mechanism of branching of the dendrites to establish the long-range arrangement of the structure along the basal plane.

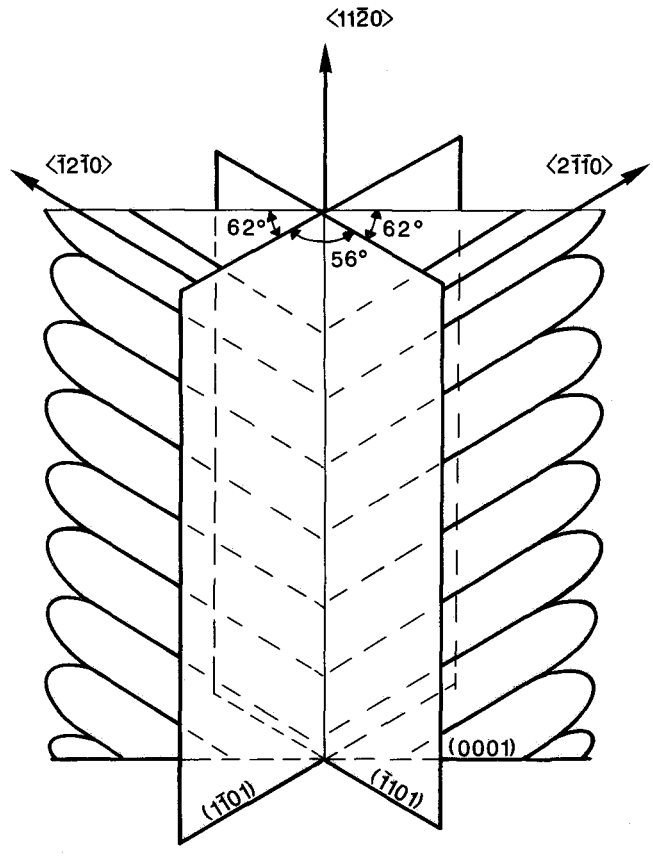

Fig. 6—Essential feature of a columnar dendrite in the magnesium alloy AZ91. The secondary arm directions in the basal plane are indicated in the figure. This is not done for the other secondary directions, because they have not yet been determined.

Weinberg and Chalmers,[6] in their study on zinc, argue that, since planes of the form $(11\bar{2}0)$ are the second most densely packed planes, the metal will form hexagons with these planes as limiting sides during solidification. This follows from Bravai's rule that the direction perpendicular to the most closely packed planes is the most slowly growing direction during crystal growth. Further growth will continue in the directions of the corners of this hexagon; thus, the dendrites will grow in the $\langle 10\bar{1}0\rangle$-directions. When grown from the vapor, pure magnesium forms crystals with well-developed faces, primarily of the (0001), $(10\bar{1}0)$, and $(10\bar{1}1)$ type.[10] Using the same arguments as Weinberg and Chalmers[6] on the present alloy, we conclude that the $\langle 11\bar{2}0\rangle$-directions are the expected dendrite directions, as also found experimentally.

IV. CONCLUSIONS

It can be concluded that the main direction of growth during directional solidification of the industrial magnesium alloy AZ91 is $\langle 11\bar{2}0\rangle$. There are six secondary arms around the primary dendrite stalk, two lying in the basal plane, and four in planes of the $(10\bar{1}1)$-type. The arms in the basal plane are of the same crystallographic direction as the primary direction, and 60 deg from the primary direction. The precise crystallographic direction of the other arms is not yet clearly established.

ACKNOWLEDGMENT

This work was supported financially by Norsk Hydro, Magnesium Division, Porsgrunn, Norway.

REFERENCES

1. M.C. Flemings: *Solidification Processing*, McGraw-Hill, Inc., New York, NY, 1974, pp. 134-74.
2. R.E. Reed-Hill: *Physical Metallurgy Principles*, van Nostrand Company, Princeton, NJ, 1964, pp. 378-85.
3. B. Chalmers: *Principles of Solidification*, John Wiley & Sons, Inc., New York, NY, 1964, pp. 116-20.
4. B. Chalmers: *Trans. AIME*, 1954, vol. 200, pp. 519-32.
5. W. Kurz and D.J. Fisher: *Fundamentals of Solidification*, Trans. Tech. Publications, 1986, pp. 7-72.
6. F. Weinberg and B. Chalmers: *Can. J. Phys.*, 1952, vol. 30, pp. 488-502.
7. D.J. Dingley: *Scanning Electron Microscopy*, 1984, vol. 2, pp. 569-75.
8. P.J. Ahearn and M.C. Flemings: *Trans. AIME*, 1967, vol. 239, pp. 1590-93.
9. T.F. Bower, H.D. Brody, and M.C. Flemings: *Trans. AIME*, 1966, vol. 236, pp. 624-34.
10. J.J. Gilman: *The Art and Science of Growing Crystals*, John Wiley & Sons, Inc., New York, NY, 1963, pp. 31-32.